molecular pharmaceutics

Article

pubs.acs.org/molecularpharmaceutics

Dual-Function Polymeric HPMA Prodrugs for the Delivery of miRNA

Zheng-Hong Peng,[†] Ying Xie,[†] Yan Wang, Jing Li, and David Oupický*

Center for Drug Delivery and Nanomedicine, Department of Pharmaceutical Sciences, University of Nebraska Medical Center, Omaha, Nebraska 68198, United States

Supporting Information

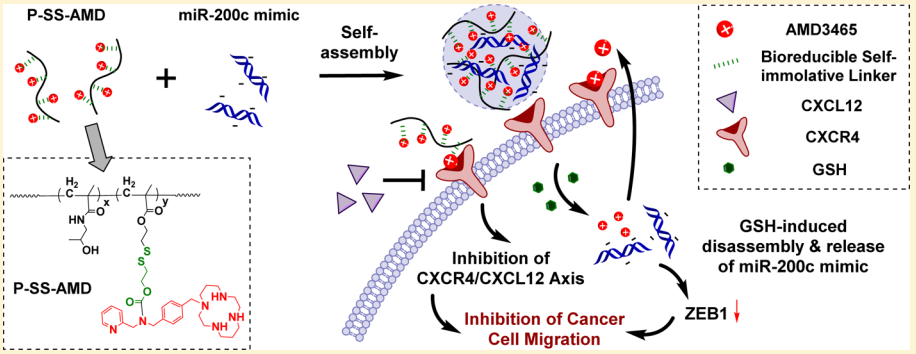

ABSTRACT: An HPMA-based polymeric prodrug of a CXCR4 antagonist, AMD3465 (P-SS-AMD), was developed as a dual-function carrier of therapeutic miRNA. P-SS-AMD was synthesized by a copolymerization of HPMA with a methacrylamide monomer in which the AMD3465 was attached via a self-immolative disulfide linker. P-SS-AMD showed effective release of the parent AMD3465 drug following treatment with intracellular levels of glutathione (GSH). The AMD3465 was released in the cells and exhibited functional CXCR4 antagonism, demonstrated by inhibition of the CXCR4-mediated cancer cell invasion. Due to its cationic character, P-SS-AMD could form polyplexes with miRNA and mediate efficient transfection of miR-200c mimics to downregulate expression of a downstream target ZEB-1 in cancer cells. The combined P-SS-AMD/miR-200c polyplexes showed improved ability to inhibit cancer cell migration when compared with individual treatments. The reported findings validate P-SS-AMD as a dual-function delivery vector that can simultaneously deliver a therapeutic miRNA and function as a polymeric prodrug of CXCR4 antagonist.

KEYWORDS: *polyplexes, miRNA delivery, polymeric prodrug, CXCR4 antagonist, self-immolative linker*

INTRODUCTION

miRNAs are a large group of small noncoding RNAs of 20−24 nucleotides that regulate gene expression by suppressing mRNA translation and reducing mRNA stability.[1] An increasing number of miRNAs have been identified as direct regulators of cancer progression and metastasis and proposed as potential therapeutics.[2,3] There are two major approaches to utilizing miRNA as therapeutics. First, miRNA mimics, which provide the same sequences as the mature endogenous target miRNA, can be delivered into cancer cells to increase the expression of tumor-suppressive miRNAs. The second approach is to use miRNA antagonists, which contain sequences complementary to the target miRNA mature strand to inhibit the activity of oncogenic miRNAs.[4,5] However, miRNA faces the same delivery challenges as other nucleic acids, which are unable to easily penetrate cell membranes due to their polar character and negative charge. Synthetic carriers such as cationic liposomes and polycations, including poly(ethylenimine) (PEI), poly(2-dimethylaminoethyl methacrylate) (PDMAEMA), guanidinium-rich polymers, and cyclodextrin-based polycations, have been developed for siRNA and DNA delivery.[6−12] Some of them, including liposomes, PEI, PDMAEMA, polylysine, and polyarginine, have also been used for miRNA delivery.[13−19]

The combination of therapeutic miRNAs and small molecule drugs has emerged as a promising strategy in cancer treatment to overcome adaptive multidrug resistance and target multiple disease pathways.[20−23] However, to achieve successful codelivery of both therapeutics requires development of an appropriate delivery platform. Not only must the vector be safe and efficient, it also needs to be versatile to accommodate the two therapeutics with distinct physicochemical characteristics. Most of the miRNA and small molecule codelivery systems simply encapsulate the drug via hydrophobic interactions in a hydrophobic part of the carrier and then incorporate the miRNA by electrostatic interactions.[14,24−28] One major disadvantage of this combination is that it is difficult to achieve a synergistic release profile of the drug and miRNA. Another

Special Issue: Bioconjugate Therapeutics

Received: November 3, 2016
Revised: December 30, 2016
Accepted: January 14, 2017
Published: January 30, 2017

DOI: 10.1021/acs.molpharmaceut.6b00999
Mol. Pharmaceutics 2017, 14, 1395−1404

disadvantage is that most of the polycations are nondegradable and produce unwanted systemic toxicities.[29]

Self-immolative spacers represent a class of linkers that can undergo spontaneous and irreversible intramolecular reaction upon stimulation.[30] They have attracted interest in the development of small-molecule and polymeric prodrugs especially in situations where the linker is sterically inaccessible or the rates of the linker cleavage and drug release are too slow.[31,32] Disulfide-based self-immolative linkers are among the most attractive linkers for developing polymers suitable for delivering drugs and imaging agents because they can be cleaved by the thiol−disulfide reaction in the intracellular reducing environment.[33−35] So far, there are no reports on the use of self-immolative disulfide spacers in miRNA delivery.

Existing evidence highlights the critical role of chemokine receptor CXCR4 and its ligand CXCL12 in cancer metastasis.[36] CXCR4 is associated with more than 23 types of human cancer.[37] CXCR4 inhibition by small molecule antagonists based on cyclam, such as plerixafor (AMD3100), can successfully block the intracellular signaling cascades that lead to cancer cell migration and invasion.[38] Monocyclam AMD3465 is another promising CXCR4 antagonist in clinical trials, with a 22-fold higher potency than AMD3100.[39,40] The protonated multiple amines in AMD3465 at physiological pH are also capable of interacting with nucleic acids, which makes it a suitable building block to design a polycationic prodrug to deliver drug and nucleic acid combinations to treat metastatic cancers.

Here we report a novel polymeric AMD3465 prodrug named P-SS-AMD that not only delivers therapeutic nucleic acids, but also inhibits the CXCR4/CXCL12 chemokine axis. CXCR4 antagonist AMD3465 was attached to a hydrophilic and nontoxic *N*-(2-hydroxypropyl) methacrylamide (HPMA)[41] copolymer via a self-immolative disulfide linker. P-SS-AMD was expected to function dually to deliver therapeutic miR-200c mimic and to release the parent drug AMD3465 following internalization into cancer cells to achieve combination cancer therapy (Scheme 1).

Scheme 1. Proposed Mechanism of Action of P-SS-AMD/miR-200c Polyplexes

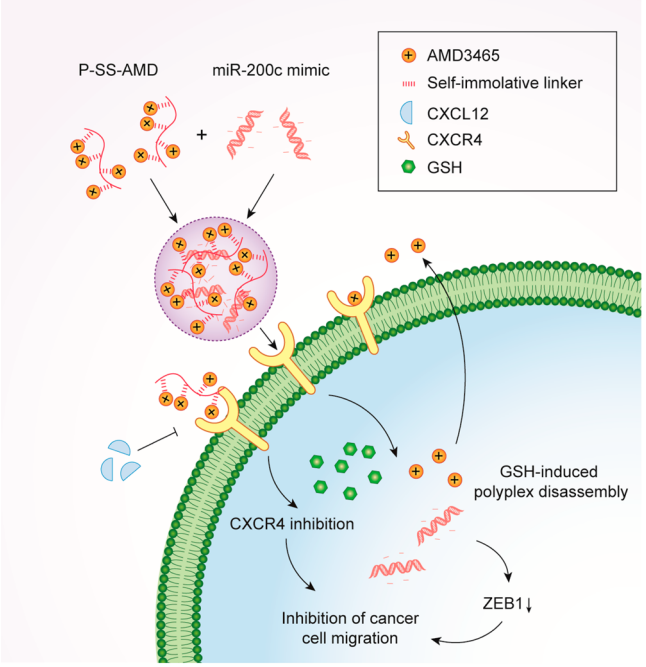

MATERIALS AND METHODS

Materials. Azobis(isobutyronitrile) (AIBN), L-glutathione (GSH), 2,2′-dichloro-*p*-xylene, 2-picolylamine, 2,2′-dithiodiethanol, methacryloyl chloride, triphosgene, and ethylenediamine tetraacetic acid (EDTA) were purchased from Sigma-Aldrich. HPMA was purchased from Amadis Chemical (Hangzhou, China). Human CXCL12 was from Shenandoah Biotechnology, Inc. (Warwick, PA). miR-200c mimic (mature miRNA sequence: 5′-UAAUACUGCCGGGUAAUGAUGGA-3′) and negative control miR-NC (mature miRNA sequence: 5′-UCACAACCUCCUAGAAAGAGUAGA-3′) were purchased from GE Dharmacon (Lafayette, CO). Oligofectamine (OligoFT) was from ThermoFisher Scientific. All the other regents were purchased from Fisher Scientific unless specifically noted.

Synthesis of MA-SS-AMD Monomer. *Synthesis of Tri-tert-butyl-1,4,8,11-tetraazacyclotetradecane-1,4,8-tricarboxylate (**2**).* Cyclam (**1**) (2.5 g, 12.5 mmol) and dichloromethane (DCM) (500 mL) were added to a round-bottom flask and cooled to 0 °C. A solution of Boc_2O (8.18 g, 37.5 mmol) in DCM (162.5 mL) was added slowly into the above solution, and the reaction mixture was allowed to warm to room temperature and stirred overnight. The mixture was then concentrated, washed with water and brine, and dried with anhydrous Na_2SO_4. The solvent was then removed under reduced pressure, and the residue was purified by flash chromatography on silica gel to obtain pure product **2** (4.46 g, 71.4%). ^{1}H NMR (500 MHz, $CDCl_3$, δ): 1.45 (s, 27H), 1.64−1.78 (m, 2H), 1.82−1.98 (m, 2H), 2.60−2.64 (m, 2H), 2.78−2.84 (m, 2H), 3.22−3.50 (m, 12H).

*Synthesis of Tri-tert-butyl 11-(4-(Chloromethyl)benzyl)-1,4,8,11-tetraazacyclotetradecane-1,4,8-tricarboxylate (**3**).* To a solution of 2,2′-dichloro-*p*-xylene (875.3 mg, 5 mmol) in acetonitrile (12.5 mL) was added anhydrous K_2CO_3 (172.8 mg, 1.25 mmol). A solution of compound **2** (500.7 mg, 1 mmol) in acetonitrile (10 mL) was added slowly into the above mixture. After stirring at reflux temperature for 6 h, the solution was filtered and concentrated. The residue was dissolved in DCM and purified by flash chromatography to obtain product **3** (530.1 mg, 83%). ^{1}H NMR (500 MHz, CD_2Cl_2, δ): 1.41 (s, 18H), 1.45 (s, 9H), 1.67 (m, 2H), 1.87 (m, 2H), 2.38 (m, 2H), 2.59 (m, 2H), 3.20−3.38 (m, 12H), 3.53 (s, 2H), 4.59 (s, 2H), 7.28−7.29 (d, J = 5 Hz, 2H), 7.32−7.33 (d, J = 5 Hz, 2H).

*Synthesis of Tri-tert-butyl 11-(4-(((Pyridin-2-ylmethyl)-amino)methyl)benzyl)-1,4,8,11-tetraazacyclotetradecane-1,4,8-tricarboxylate (**4**).* Anhydrous K_2CO_3 (207.3 mg, 1.5 mmol), acetonitrile (5 mL), compound **3** (639.3 mg, 1 mmol), and 2-picolylamine (1.08 g, 10 mmol) were added successively into a round-bottom flask and stirred at room temperature overnight. Then the solid was filtered and the filtrate was concentrated. The remaining residue was dissolved in DCM, and the solution was washed with water and brine and dried with anhydrous Na_2SO_4. After concentration, the crude product was purified by flash chromatography and pure product **4** (579.4 mg, 81.5%) was obtained. ^{1}H NMR (500 MHz, d_6-DMSO, δ): 1.30 (s, 18H), 1.40 (s, 9H), 1.60 (m, 2H), 1.81 (m, 2H), 2.30 (m, 2H), 2.52 (m, 2H), 3.16−3.25 (m, 12H), 3.48 (s, 2H), 3.71 (s, 2H), 3.78 (s, 2H) 7.20−7.22 (d, J = 10 Hz, 2H), 7.24 (d, 1H), 7.26−7.28 (d, J = 10 Hz, 2H), 7.44 (d, 1H), 7.73−7.76 (d, 1H), 8.5 (d, 1H).

DOI: 10.1021/acs.molpharmaceut.6b00999
Mol. Pharmaceutics 2017, 14, 1395−1404

*Synthesis of 2-((2-Hydroxyethyl)disulfanyl)ethyl Methacrylate (**5**).* 2,2′-dithiodiethanol (6.16 g, 40 mmol), anhydrous tetrahydrofuran (THF) (200 mL), and triethylamine (TEA) (6.07 g, 60 mmol) were added to a 1 L round-bottom flask and cooled to 0 °C. Then methacryloyl chloride (4.18 g, 40 mmol) in 100 mL of anhydrous THF was added dropwise into the above solution. The reaction mixture was warmed to room temperature and stirred overnight. The precipitation was filtered, and the collected solution was concentrated. The residue was dissolved in ethyl acetate, washed with water and brine, and dried over anhydrous Na_2SO_4. The crude product was purified by silica gel column chromatography using ethyl acetate/hexane as the eluent. Pure product **6** (5.62 g) was obtained with a yield of 63.2%. ^{1}H NMR (500 MHz, $CDCl_3$, δ): 1.95 (s, 3H), 2.88−2.90 (t, J = 5 Hz, 2H), 2.97−2.99 (t, J = 5 Hz, 2H), 3.89−3.92 (t, J = 5 Hz, 2H), 4.41−4.43 (t, J = 5 Hz, 2H), 5.60 (s, 1H), 6.14 (s, 1H).

*Synthesis of Tri-tert-butyl 11-(4-(13-Methyl-3,12-dioxo-2-(pyridin-2-ylmethyl)-4,11-dioxa-7,8-dithia-2-azatetradec-13-en-1-yl)benzyl)-1,4,8,11-tetraazacyclotetradecane-1,4,8-tricarboxylate (MA-SS-AMD, **6**).* Compound **5** (855.2 mg, 3.85 mmol), triphosgene (380.5 mg, 1.28 mmol), and TEA (537 μL) in DCM (10 mL) were stirred at −65 °C for 2 h. Then, a solution of compound **4** (2.735 g, 3.85 mmol) and TEA (537 μL) in DCM (10 mL) was added and stirred overnight. The mixture was washed with water and brine and dried with anhydrous Na_2SO_4. After concentration under reduced pressure, the crude product was purified by flash chromatography (DCM/MeOH) to give the pure product **7** (2.36 g, 64%). The calculated mass of $[M + H]^+$ was 959.5, and the found mass was 959.2. ^{1}H NMR (500 MHz, CD_2Cl_2, δ): 1.41 (s, 18H), 1.44 (s, 9H), 1.62−1.68 (m, 2H), 1.82−1.99 (m, 2H), 1.91 (s, 3H), 2.3−2.4 (m, 2H), 2.52−2.62 (m, 2H), 2.85−3.02 (m, 4H), 3.18−3.38 (m, 12H), 3.52 (s, 2H), 4.30−4.44 (m, 4H), 4.46−4.54 (m, 4H), 5.56 (s, 1H), 6.08 (s, 1H), 7.15−7.25 (m, 6H), 7.62−7.66 (dd, 1H), 8.50−8.51 (d, 1H).

Synthesis and Characterization of P-SS-AMD. HPMA (103.6 mg, 0.72 mmol), MA-SS-AMD (**6**) (347 mg, 0.36 mmol), AIBN (11.3 mg), and DMF (2 mL) were added into a 5 mL ampule. After bubbling with nitrogen for 30 min, the ampule was sealed and the mixture was heated at 50 °C for 24 h. The polymer was precipitated into cold diethyl ether, centrifuged, and dried in air for 4 h. The dried polymers were mixed with trifluoroacetic acid (10 mL) and stirred at room temperature for 3 h. After trifluoroacetic acid was removed under reduced pressure, the remaining polymer solution was precipitated by dropwise addition into cold diethyl ether. The polymer was isolated by filtration, dried in vacuum, and then dissolved in water and dialyzed against 1 M HCl followed by final lyophilization. The molecular weights and molecular weight distribution of the polymers were determined by size-exclusion chromatography (TSK-GEL PW_{XL} column, Toshoh Bioscience) equipped with a miniDAWN TREOS multi-angle static light scattering detector (Wyatt) and Optilab T-rEX differential refractive index detector (Wyatt) using 0.5 M sodium acetate buffer (pH 5) as the mobile phase.

Drug Release Kinetics. P-SS-AMD (2.5 mg) was dissolved in 1.5 mL of phosphate buffer (100 mM potassium phosphate, 1 mM EDTA, pH 7.4) and incubated with or without 10 mM GSH at 37 °C. The released AMD3465 in the solution was measured at 254 nm on an analytical HPLC column (Eclipse plus C18, 5 μm, 4.6 × 150 mm) every 30 min during the first 24 h and every 12 h in the following 36 h. The elute gradient was increased from 5% buffer B to 95% buffer B (buffer A, 0.1% TFA in water; buffer B, 0.1% TFA in acetonitrile) in 20 min, and the flow rate was 1 mL/min. The experiment was repeated three times. AMD3465 was used as the reference.

Gel Retardation Assay. Polyplexes were prepared by adding a predetermined volume of P-SS-AMD or AMD3465 to a miRNA solution (20 μM in 10 mM HEPES pH 7.4) to achieve the desired w/w ratio and vigorously vortexed for 10 s. Polyplexes were then incubated at room temperature for 30 min before further use. Some polyplexes were also incubated with 10 mM GSH for 24 h. Each sample (7.5 μL) was then mixed with 1.5 μL of a loading buffer (Ambion, USA) before loading to 2% agarose gel. The gel was developed at 120 V for 30 min in a running buffer (40 mM Tris-HCl, 1 v/v% acetic acid, 1 mM EDTA) containing 0.5 μg/mL ethidium bromide. The miR-200c bands were detected using an EL LOGIC100 imaging system (Kodak, USA).

Polyplex Size and Surface Charge. The average hydrodynamic diameter and surface charge of polyplexes were determined by dynamic light scattering (Zetasizer Nano Series, Malvern). miR-200c mimic (4 μL, 100 μM) was mixed with P-SS-AMD at different amine-to-phosphate (N/P) ratios in HEPES buffer (10 mM, pH 7.4) for 30 min and then diluted to 1 mL with the same HEPES buffer. Some polyplexes were incubated with 10 mM GSH for 24 h. All measurements were conducted in automatic mode at room temperature at 173° scattering angle.

Cell Culture. Human osteosarcoma cells (U2OS) stably expressing human CXCR4 receptor fused to the N-terminus of enhanced green fluorescent protein (EGFP) were purchased from Fisher Scientific and cultured in Dulbecco's modified Eagle's medium high glucose medium supplemented with 10% fetal bovine serum (FBS), 2 mM L-glutamine, 1% Pen-Strep, and 500 μg/mL G418 in an incubator at 37 °C and 5% CO_2.

Cytotoxicity. In vitro cytotoxicity of P-SS-AMD in U2OS cells was examined using the CellTiter-Blue cell viability assay (Promega). The cells were plated in 96-well microplates at a density of 5000 cells/well and treated with P-SS-AMD diluted in culturing medium for 24 h. The medium was then removed and replaced with a mixture of 100 μL of serum-free medium and 20 μL of CellTiter-Blue reagent. After 2 h of incubation, the fluorescence intensity $[I]$ was measured using SpectraMaxM5e Multi-Mode microplate reader (Molecular Devices, CA) at $560_{Ex}/590_{Em}$. Relative cell viability (%) was calculated as $[I]_{treated}/[I]_{untreated} \times 100\%$. To confirm that the polyplex formulation used in transfection and cell migration is within the safe dosing range, cells were plated as described before and treated with PBS, OligoFT/miR-NC, OligoFT/miR-200c, P-SS-AMD/miR-200c, or P-SS-AMD/miR-200c. After 48 h of incubation, the medium was removed and cell viability was measured as described before.

CXCR4 Antagonism. The U2OS cells were seeded at a density of 8,000 cells per well 24 h prior to treatment. Cells were washed twice with PBS and incubated in HEPES-buffered DMEM medium containing 1% FBS with AMD3465 and P-SS-AMD (with or without 24 h of GSH pretreatment) for 30 min before exposure to CXCL12 (10 nM) for another 1 h. The cells were then fixed with 4% paraformaldehyde and washed four times with PBS, and nuclei were stained with 1 μM Hoechst 33258 solution for 30 min before imaging. Images were taken by EVOS FL microscope at 20× magnification. High-content analysis was applied to quantify the CXCR4 antagonistic activity based on the internalization of the EGFP-CXCR4

DOI: 10.1021/acs.molpharmaceut.6b00999
Mol. Pharmaceutics 2017, 14, 1395−1404

Scheme 2. Synthesis of P-SS-AMD Polymeric Prodrugs

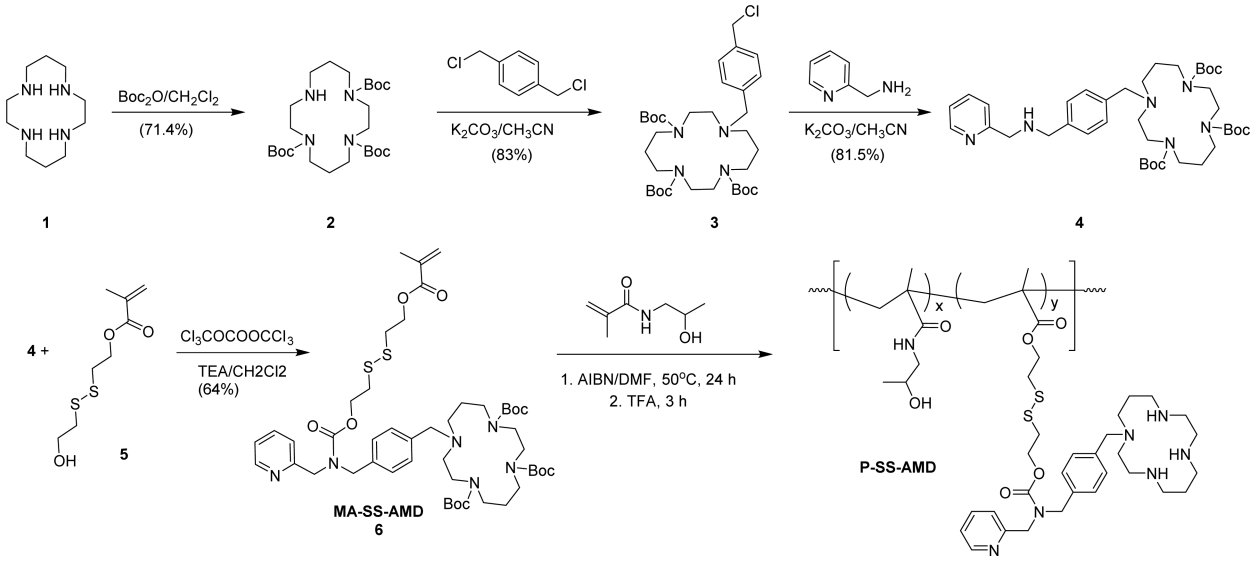

receptors from plasma membrane into the cells. Cellomics Arrayscan VTI fluorescent microscope imager (Thermo Fisher) was used for the imaging and analysis.[42] Untreated cells stimulated with CXCL12 were used as negative control (0% CXCR4 antagonism), and cells treated with 300 nM AMD3100 were used as positive control (100% CXCR4 antagonism).

Cellular Uptake. U2OS cells were seeded in 6-well plates at a density of 500,000 cells per well and cultured for 24 h prior to treatment. The cells were incubated with polyplexes prepared at different N/P ratios using P-SS-AMD and AlexaFluor555 labeled double-stranded oligonucleotides Alexa Red-Oligo (BLOCK-iT Alexa Fluor Red Fluorescent Control, catalog number 14750100, ThermoFisher Scientific) in serum-free medium for 4 h. The cells were then detached from the plate after being incubated with TrypLE (ThermoFisher Scientific) for 3 min and collected for flow cytometry analysis using BD FACSCalibur. Data were processed and analyzed using FlowJo software V7.6.1.

miRNA Transfection. U2OS cells were seeded 24 h prior to transfection to reach logarithmic growth phase. On the day of transfection, cells were incubated with polyplexes prepared with either miR-200c or miR-NC at various N/P ratios in serum-free medium. After 4 h incubation, polyplexes were completely removed and replaced with culture medium with 10% FBS for 48 h prior to RT-PCR analysis. Total RNA was extracted from the transfected U2OS cells using mirVana miRNA isolation kit (Ambion, USA) according to the manufacturer's protocol. The quantification of mature miR-200c using TaqManMicroRNA assay included a two-step RT-PCR. First, 10 ng of RNA from each sample was converted to cDNA using TaqMan microRNA reverse transcription cDNA synthesis kit (Applied Biosystems, California) with specific primers for miR-200c or internal reference Z30 (Applied Biosystems, California) according to the manufacturer's protocol. Second, the PCR amplification of target cDNA was performed on Rotor-Gene Q qPCR instrument (QIAGEN) with specific primers for miR-200c or Z30 using AmpliTaq Gold enzymes. The expression of miR-200c level was normalized to internal miRNA reference Z30 using comparative C_T method.

Western Blot. The ZEB1 levels in U2OS cells were quantified with Western blot. After transfection with the miR-200c or miR-NC polyplexes for 48 h, the cells were washed twice with PBS and lysed in radioimmunoprecipitation assay buffer (RIPA) buffer containing 1× protease inhibitor cocktail (Thermo Scientific) for 10 min on ice. The mixture was centrifuged, and the supernatant was collected. After measuring the protein concentration with bicinchoninic acid protein assay (Pierce), the total protein samples (20 μg) were separated on a 10% SDS−PAGE gel run at 120 V for 2 h. Then the proteins were transferred to the nitrocellulose membrane at a constant current of 300 mA for 2 h. After confirming the transfer efficiency and blocking the membranes with 5% nonfat milk, the membrane was probed by human ZEB1 mAb (Cell Signaling Technology, USA) followed by incubation with secondary rabbit IgG HRP-linked antibody (Cell Signaling Technology, USA). After the membrane was incubated with Pierce ECL Western blot detection reagent (Thermo Scientific, USA) for 1 min, the film was developed on the medical film processor (Konica Minolta Medical & Graphic Inc.). Finally, the film was scanned and the intensity of the protein bands was quantified by ImageJ software (NIH).

Cell Migration Assay. U20S cells (2×10^5) were seeded into 6-well plates and cultured in complete DMEM for 24 h before transfection. The cells were subsequently treated with PBS, OligoFT/miR-NC, Oligofectamine/miR-200c, P-SS-AMD/miR-NC, and P-SS-AMD/miR-200c. After 48 h incubation, the cells were trypsinized and suspended in medium without serum. Subsequently, 3×10^4 cells were seeded in the top chambers in 300 μL of serum-free medium and 500 μL of complete medium containing 10% FBS was added to the lower Transwell chambers. After 12 h, the nonmigrated cells in the top chamber were removed with a cotton swab. The migrated cells were fixed in 100% methanol and stained with 0.2% Crystal Violet solution for 10 min at room temperature. The images were taken by EVOS XL microscope. Three 20× visual fields were randomly selected for each insert, and each group was conducted in triplicate.

DOI: 10.1021/acs.molpharmaceut.6b00999
Mol. Pharmaceutics 2017, 14, 1395−1404

RESULTS AND DISCUSSION

Synthesis of Polymeric Prodrug Based on AMD3465 (P-SS-AMD). The key procedure to synthesize the polymeric prodrug P-SS-AMD with the self-immolative linker was to develop the reactive monomer MA-SS-AMD (Scheme 2). We designed a concise synthetic scheme that protects the amines on the cyclam ring because of their critical function in binding with the CXCR4 receptor.[39] Three of the four cyclam (**1**) amines were protected with di-*tert*-butyl dicarbonate to give **2** with 71% yield.[43] The protected cyclam (**2**) was reacted with α,α'-dichloro-*p*-xylene to afford the benzyl chloride (**3**) at 83% yield. The benzyl chloride in **3** was subsequently substituted with 2-picolylamine to prepare Boc-protected AMD3465 (**4**) in 82% yield. Methacryloylation of 2-hydroxyethyl disulfide afforded the corresponding alcohol (**5**),[34] which was then reacted with triphosgene and **4** to give the desired monomer MA-SS-AMD (**6**). The monomer was analyzed by ^{1}H NMR (Figure S1) and mass spectroscopy. The calculated mass of the MA-SS-AMD monomer (**6**) ($[M + H]^+$) was 959.5, and the found mass was 959.2.

The presence of the disulfide bond in the monomer MA-SS-AMD has the potential to interfere with reversible addition−fragmentation transfer polymerization due to the thiol−disulfide exchange.[44] Thus, we have used conventional free radical polymerization to prepare the polymer prodrug P-SS-AMD. As shown in Scheme 2, P-SS-AMD was synthesized by a two-step reaction. First, MA-SS-AMD was copolymerized with HPMA in DMF at 50 °C for 24 h. Following isolation of the polymer by precipitation in diethyl ether, the Boc protecting groups were removed from the cyclams by trifluoroacetic acid. The final polymer was dialyzed against water acidified with 1 M HCl to remove residual monomers and other low molecular weight impurities. Acidified water was used to enhance solubility of the monomers during dialysis and to convert the final polymer into hydrochloride salt. The molecular weight and molecular weight distribution of the synthesized copolymer were determined by size exclusion chromatography. The number-average molecular weight (M_n) was 27.8 kDa, and the polydispersity index (PDI, M_w/M_n) was 2.2. The calculated mol % of the MA-SS-AMD comonomer in the polymer was 31%, which was close to the 33% in the feed. The weight content of AMD3465 in the P-SS-AMD was 22.1%, which was calculated based on the ^{1}H NMR data (Figure S2).

AMD3465 Release from P-SS-AMD. We have selected the disulfide-based self-immolative linker because of the specific cellular location of its activation. Disulfide bonds are preferentially cleaved by GSH in the reducing intracellular environment typically found in the cytoplasm (Scheme 1). The cytoplasmic location of the linker cleavage is ideally suited for delivery and release of therapeutic miRNA because cytoplasm is the site of miRNA activity. The mechanism of GSH-triggered drug release is shown in Figure 1A. Reaction with GSH thiolate initiates a release cascade of the parent drug AMD3465 from P-SS-AMD via thiolactone formation and subsequent amide bond cleavage. The kinetics of the linker cleavage was measured by incubating the polymer with 10 mM GSH at 37 °C to mimic the elevated intracellular GSH levels in cancer cells. The drug release was monitored by an analytical HPLC system. The HPLC profile of polymer P-SS-AMD is shown in Figure S3A. A new peak appeared at 5.36 min in Figure S3B, which was confirmed by mass spectrometry to be the released parent product AMD3465 (Figure S4). The release kinetics (Figure 1B) shows that over 90% of AMD3465 was released from the polymer upon incubation with GSH within 24 h. In contrast, in the absence of GSH there was less than 1% of the AMD3465 released even after 60 h.

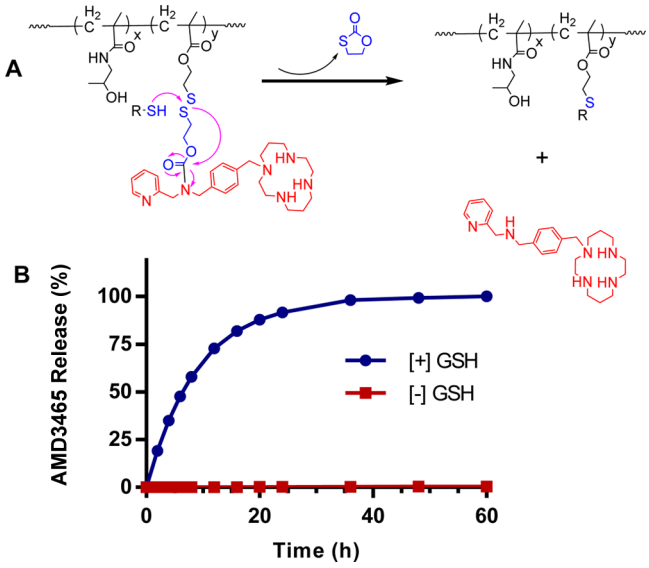

Figure 1. (A) Proposed release mechanism and (B) cumulative release of AMD3465 from P-SS-AMD with 10 mM GSH.

Cytotoxicity. Before evaluating miRNA delivery and biological activity of P-SS-AMD, we tested the cytotoxicity to determine the safe concentration range for subsequent studies in U2OS cells (Figure S5). The cells were treated with increasing concentrations of P-SS-AMD in culture medium before measuring cell viability, and the estimated IC50 for P-SS-AMD was 82 μg/mL. Safe concentrations of P-SS-AMD were selected and applied in all the subsequent cell-based experiments.

CXCR4 Antagonism. We have shown in Figure 1 that the parent drug AMD3465 can be successfully released from P-SS-AMD. It was then important to test if the intracellularly released drug retains its CXCR4 antagonism. We examined the CXCR4 antagonism using U2OS cells that are stably expressing CXCR4 receptor tagged with EGFP. High-content analysis was applied to quantify the antagonism activity and calculate the EC_{50} as described in our previous publications.[42] Control small molecule CXCR4 antagonist AMD3100 (300 nM) was used as a positive control and set as 100%. To comprehensively assess the CXCR4 activity of the polymeric prodrug, we constructed dose−response curves and determined EC_{50} values for AMD3465 and P-SS-AMD (with and without GSH) (Figure 2A). AMD3465 exhibited EC_{50} of 0.3 nM, indicating high potency in CXCR4 inhibition. As expected, P-SS-AMD demonstrated lower activity in CXCR4 inhibition with an EC_{50} of 54.9 nM (expressed as molar concentration of AMD3465 units in the polymer). When P-SS-AMD was pretreated with GSH before incubation with the cells, however, the EC_{50} was decreased to 5 nM, confirming enhanced potency for CXCR4 antagonism when exposing the receptor directly from the extracellular space. We then assessed CXCR4 inhibition at a concentration expected to be used in the subsequent miRNA delivery experiments. As shown in Figure 2B, AMD3465 exhibited complete CXCR4 inhibition at 300 nM concentration. Even though P-SS-AMD showed a somewhat lower inhibitory activity when tested at the equivalent

DOI: 10.1021/acs.molpharmaceut.6b00999
Mol. Pharmaceutics 2017, 14, 1395−1404

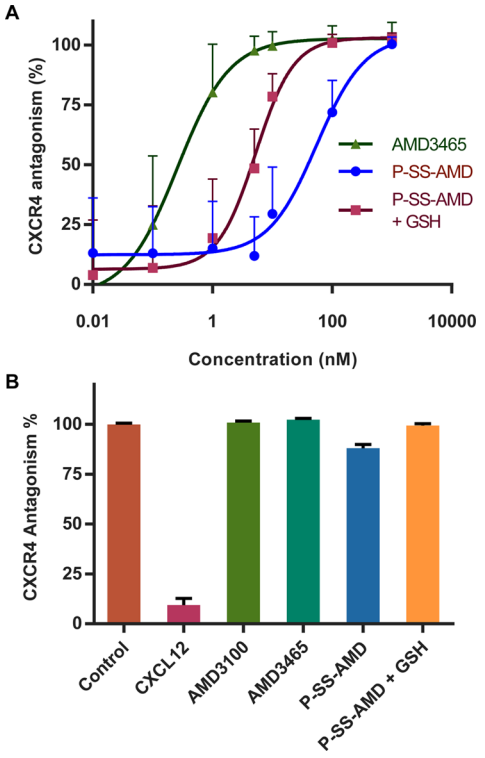

Figure 2. CXCR4 antagonism of P-SS-AMD by CXCR4 redistribution assay. (A) Dose−response curve of P-SS-AMD3465 (± GSH) and AMD3465. (B) % CXCR4 antagonism at 300 nM AMD3465 equiv.

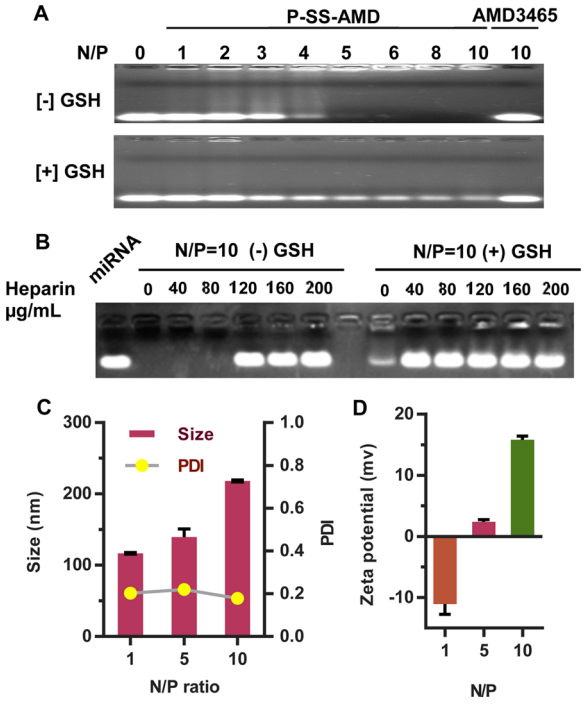

Figure 3. Physicochemical properties of P-SS-AMD/miR-200c polyplexes. (A) Gel retardation assay of polyplexes prepared at different N/P ratios of miR-200c mimic and P-SS-AMD or free AMD3465 without and with 10 mM GSH. (B) Heparin- and GSH-induced miRNA release from P-SS-AMD/miRNA (N/P 10). Polyplexes were incubated with increasing concentrations of heparin either with or without 20 mM GSH for 30 min. (C) Hydrodynamic diameters and PDI of P-SS-AMD/miR-200c polyplexes (N/P 10). (D) Zeta potential of P-SS-AMD/miR-200c polyplexes (N/P 10).

AMD3465 concentration, it still achieved nearly complete CXCR4 inhibition (85%). When P-SS-AMD was pretreated with GSH before incubation, the antagonistic activity further increased to ∼95%. It is worth noting that despite the decrease of activity in the polymer, P-SS-AMD still exhibited CXCR4 inhibition within nM range, which falls well below the doses to be used in the miRNA delivery. These findings suggest that AMD3465 released from P-SS-AMD in the intracellular space is likely released from the cells and binds cell surface CXCR4 or binds the CXCR4 receptor as it recycles through the cell. When combined with our previously published findings, the results with GSH pretreatment also point to the possibility that P-SS-AMD exhibits CXCR4 inhibition both as AMD3465 prodrug and as a polymeric drug (i.e., P-SS-AMD itself binds and inhibits CXCR4).[42,45]

Reversible Complexation of miRNA with P-SS-AMD. After confirming that P-SS-AMD retained the CXCR4 activity of AMD3465, we set to evaluate the ability of the polymer to condense miRNA. Condensation of nucleic acids by polycations is the first requirement for their successful use as delivery vectors. The ability of P-SS-AMD to complex miR-200c into polyplexes was first evaluated by agarose gel retardation assay. Polyplexes were prepared by adding P-SS-AMD to miRNA solution at increasing N/P ratios as shown in Figure 3A. The migration of miR-200c in the gel was completely retarded at N/P ratios greater than 5. Control small molecule AMD3465 failed to complex the miRNA even at N/P 10. The reversibility of the complexation was assessed by the addition of 10 mM GSH to the polyplexes (Figure 3A). After 24 h incubation in the reducing GSH conditions, the polyplexes prepared at low N/P ratios (N/P ≤ 3) disassembled because of the cleavage of the self-immolative linker and free miRNA was released completely. Polyplexes prepared at higher N/P ratios displayed only partial miRNA release, indicating incomplete disulfide cleavage in P-SS-AMD/miRNA polyplexes. Because of the partial release, we performed the release study also upon exposure to higher concentration GSH (20 mM) and heparin to assist in fully disassembling the polyplexes. As shown in Figure 3B, in the absence of GSH, the polyplexes were stable and released no miRNA until the heparin concentration exceeded 80 μg/mL. However, when incubated with 20 mM GSH, rapid disulfide reduction destabilized the polyplexes, which resulted in the partial release of miRNA even without the addition of heparin and complete release with the addition of heparin as low as 40 μg/mL. These results confirmed that P-SS-AMD can form polyplexes with miRNA and that the miRNA can be released from the polyplexes after the disulfide bonds between AMD3465 and the HPMA backbone were cleaved by GSH.

The hydrodynamic diameters of P-SS-AMD/miR-200c polyplexes prepared at N/P = 1, 5, and 10 were 116.6 ± 2.4, 139.4 ± 19.9, and 218.2 ± 2.7 nm, respectively, with polydispersity indices of 0.203, 0.220, and 0.179, respectively (Figure 3C). Particle size is a key parameter that determines the in vivo fate of polyplexes. We know from previous studies that nanoparticles with sizes less than 200 nm are regarded as suitable for tumor delivery. Thus, the size of the P-SS-AMD polyplexes is expected to be suitable for miRNA delivery in vivo, although other parameters, like zeta potential, will also influence the efficacy of the miRNA delivery. The zeta potential of polyplexes increased from −11.1 ± 1.6 to 2.4 ± 0.3 and to 15.8 ± 0.6 (mV) when the N/P ratio of P-SS-AMD to miR-

DOI: 10.1021/acs.molpharmaceut.6b00999
Mol. Pharmaceutics 2017, 14, 1395−1404

200c increased from 1 to 10 (Figure 3D). These results further confirmed that the P-SS-AMD can form nanosized polyplexes with miRNA.

Cellular Uptake of miRNA Polyplexes. Polyplexes with positive surface charge can facilitate cellular uptake of a wide range of nucleic acids. The ability of P-SS-AMD polyplexes to deliver nucleic acids in U2OS cells was evaluated by flow cytometry and confocal microscopy using double-stranded RNA oligomer Alexa Red-Oligo labeled with AlexaFluor555. We have used the double-stranded RNA oligomer as a model of miRNA because of its commercial availability and similar structure and molecular weight with the miR-200c mimic. Polyplexes were prepared at different N/P ratios up to 10, established as safe in the cytotoxicity studies. As shown in Figure 4, cells treated with P-SS-AMD polyplexes exhibited

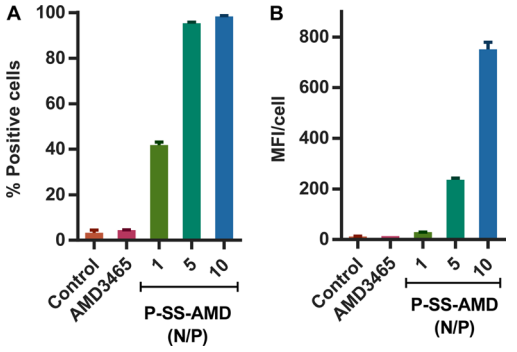

Figure 4. Cellular uptake of polyplexes. (A) Fraction of cells that internalized the polyplexes and (B) mean fluorescent intensity (MFI) per cell. U2OS cells were treated with polyplexes prepared with different N/P ratios of P-SS-AMD and Alexa Red-Oligo. Data are presented as mean ± SD (n = 3).

significant cell uptake, indicated by both enhanced fraction of fluorescent cells (Figure 4A) and mean fluorescent intensity (MFI) per cell (Figure 4B). The use of polyplexes prepared at higher N/P ratios resulted in higher cell uptake. At the highest N/P tested, nearly all cells (>97.5%) showed internalization of the polyplexes. In contrast, small molecule AMD3465 failed to facilitate any appreciable cell uptake of the fluorescently labeled oligonucleotide.

miRNA Transfection. Transfection efficiency of P-SS-AMD/miR-200c polyplexes was evaluated by measuring the levels of miR-200c in U2OS cells using RT-PCR (Figure 5). Control polyplexes prepared with negative control miRNA (miR-NC) were also included to exclude any nonspecific effects of miRNA and the polymer on miR-200c expression. miR-200c mimics were selected as the therapeutic miRNA to test delivery efficiency of P-SS-AMD as miR-200c was found to be significantly downregulated in metastatic osteosarcoma tissue specimens when compared to normal bone samples.[46] The downregulation of miR-200c resulted in the high expression of Zinc-finger E-box-binding 1 (ZEB1), which is a transcription repressor factor that has been identified as one of the powerful inducers of epithelial−mesenchymal transition and cancer metastasis.[47,48] Studies have demonstrated that successful delivery of miR-200c mimics can lead to downregulation of ZEB1 followed by inhibition of cancer migration and invasion.[45,49,50] First, our results showed that cells transfected with P-SS-AMD/miR-200c polyplexes exhibited highly elevated miR-200c levels when compared with cells treated with a mixture of AMD3465 and miR-200c (Figure 5A). When

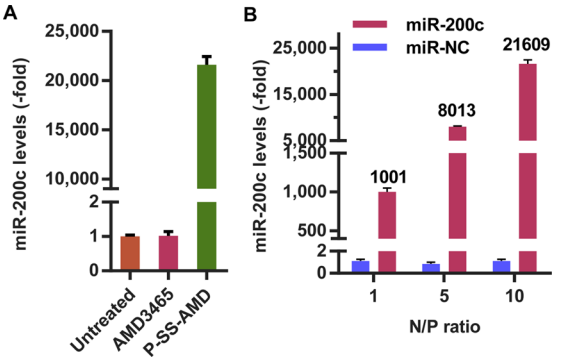

Figure 5. Transfection efficiency of P-SS-AMD/miR-200c polyplexes in U2OS cells. (A) Cells were transfected with miR-200c mimics using free AMD3465 and polymer P-SS-AMD at N/P 10. (B) Cells were transfected with different N/P ratios of P-SS-AMD polyplexes with miR-200c or miR-NC. Data are shown as mean ± SD (n = 3).

prepared at N/P 10, P-SS-AMD exhibited a more than 21,000-fold increase in the miR-200c levels over background cellular expression, while the AMD3465/miR-200c treatment had no significant effect. In addition, as shown in Figure 5B, increasing the N/P ratios of P-SS-AMD/miR-200c polyplexes resulted in significant enhancement in miR-200c levels, which was consistent with the cell uptake results above. Treatment with P-SS-AMD/miR-NC polyplexes had no effect on miR-200c expression.

After confirming that P-SS-AMD can effectively deliver miRNA, we further evaluated the effect of the delivered miR-200c on one of its important downstream targets, ZEB1. Western blot was used to analyze the cellular levels of ZEB1 after treatment with P-SS-AMD/miR-200c polyplexes. As shown in Figure 6, delivery of miR-200c with P-SS-AMD polyplexes at N/P 10 resulted in a substantial downregulation (53%) of ZEB1 in the U2OS osteosarcoma cells. In contrast, control miR-NC polyplexes showed negligible effect on ZEB1 protein expression. At lower N/P ratio (N/P 5), the extent of ZEB1 downregulation by P-SS-AMD/miR-200c polyplexes was less pronounced as only 28% downregulation was observed.

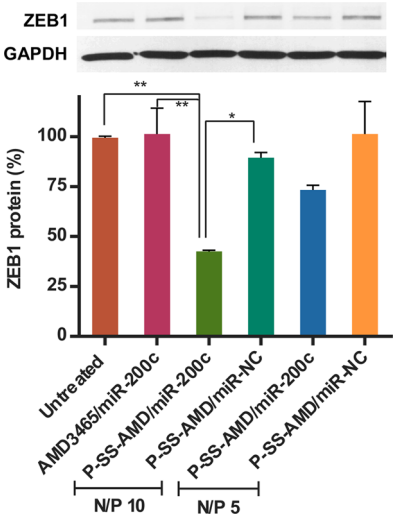

Figure 6. Effect of P-SS-AMD/miR-200c polyplexes on ZEB1 protein expression. The cells were transfected with polyplexes prepared at N/P 5 and 10 and ZEB1 levels quantified by Western blot (one-way ANOVA, *p < 0.05; **p < 0.01).

DOI: 10.1021/acs.molpharmaceut.6b00999
Mol. Pharmaceutics 2017, 14, 1395−1404

This result further confirmed that miR-200c could be efficiently delivered by the P-SS-AMD polyplexes into the U2OS cells and released successfully into the cytoplasm to regulate the miRNA downstream signaling pathways.

Effect of Combined CXCR4 Inhibition and miR-200c Delivery on Cancer Cell Migration. Both CXCR4 and downstream miR200c targets are involved in cancer metastasis. Thus, we conducted Transwell cell migration assay to examine whether the successful delivery of miR-200c using the dual-functional P-SS-AMD and its CXCR4 antagonistic activity can inhibit the migration of U2OS cells. Cells were treated with either P-SS-AMD/miR-200c polyplexes or commercial transfection agent Oligofectamine (OligoFT) for 48 h before conducting Transwell cell migration assay. As shown in Figure 7, FBS induced a significant amount of cell migration.

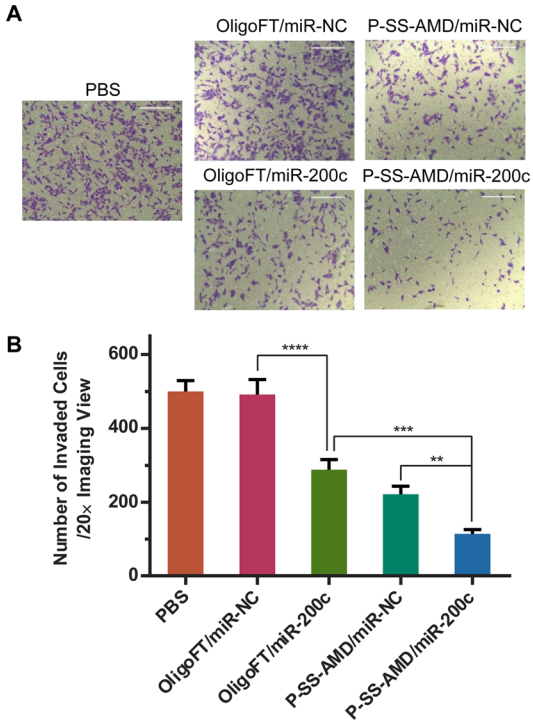

Figure 7. Inhibition of cancer cell migration by P-SS-AMD/miR-200c polyplexes. U2OS cells were transfected with either miR-200c or miR-NC polyplexes and allowed to migrate through porous membrane for 12 h toward 10% FBS. (A) Representative images of invaded cells at 20× magnification. (B) Average number of invaded cells per 20× imaging view (n = 3, ANOVA, $^{**}p < 0.01$, $^{***}p < 0.001$, $^{****}p < 0.0001$).

OligoFT/miR-200c showed about 42% inhibition of migration, while OligoFT/mi-NC showed no significant effect, confirming the antimetastatic potential of miR-200c. In contrast, P-SS-AMD/miR-NC polyplexes exhibited 56% inhibition of cell migration due to the CXCR4 antagonistic activity of the polymer prodrug. The combined P-SS-AMD/miR-200c polyplexes further enhanced the migration inhibition to 77%.

The observed inhibitory effect could be attributed to the combined activity of the CXCR4 antagonism of P-SS-AMD and the effect of miR-200c on ZEB1, which plays a critical role in inhibiting cancer cell migration. For the mechanism of action of the polyplex formulations in this study, we propose that the polyplex and free polymer P-SS-AMD both contribute to CXCR4 antagonism (Scheme 1). Typical polyplexes are prepared with excess polycation to fully condense the nucleic acids. As a result, polyplex formulations are a mixture of the actual polyplexes and excess free polymer. Based on our previous studies and findings in Figure 2, we propose that both the polyplex and free polymer P-SS-AMD antagonize the CXCR4 receptor. There is also the possibility that a small amount of the polymer is dissociated from the polyplexes upon binding to the cell surface and that partial GSH-mediated reduction occurs in the extracelullar space as well. Further, to rule out the effect of cytotoxicity on the observed cell migration data, we examined the cytotoxicity of all the formulations tested, and no cytotoxicity was observed 48 h post-transfection (Figure S6).

CONCLUSION

We have developed a novel dual-function polymeric prodrug using self-immolative linker chemistry and CXCR4 antagonist AMD3465. The dual-function polymers could effectively inhibit the CXCR4 chemokine receptor and degrade into safe HPMA copolymers. Due to their polycationic character, the polymeric prodrug could form nanosized polyplexes with miRNA and effectively deliver the nucleic acid to cancer cells. The developed delivery methodology may provide a new direction for developing approaches for drug−nucleic acid combination therapies.

ASSOCIATED CONTENT

Supporting Information

The Supporting Information is available free of charge on the ACS Publications website at DOI: 10.1021/acs.molpharmaceut.6b00999.

^{1}H NMR, HPLC, MS, and cytotoxicity results (PDF)

AUTHOR INFORMATION

Corresponding Author

*E-mail: david.oupicky@unmc.edu.

ORCID

Zheng-Hong Peng: 0000-0001-9783-5108

David Oupický: 0000-0003-4710-861X

Author Contributions

†Z.-H.P. and Y.X. contributed equally.

Notes

The authors declare no competing financial interest.

ACKNOWLEDGMENTS

This work was supported in part by the University of Nebraska Medical Center and in part by grants from the National Institutes of Health (EB015216, EB020308, EB019175). Support from the China Scholarship Council for Ying Xie is gratefully acknowledged.

REFERENCES

(1) Svoronos, A. A.; Engelman, D. M.; Slack, F. J. OncomiR or Tumor Suppressor? The Duplicity of MicroRNAs in Cancer. *Cancer Res.* **2016**, *76*, 3666−70.

(2) Jansson, M. D.; Lund, A. H. MicroRNA and cancer. *Mol. Oncol.* **2012**, *6*, 590−610.

(3) Bouyssou, J. M. C.; Manier, S.; Huynh, D.; Issa, S.; Roccaro, A. M.; Ghobrial, I. M. Regulation of microRNAs in cancer metastasis. *Biochim. Biophys. Acta, Rev. Cancer* **2014**, *1845*, 255−265.

(4) Peng, B.; Chen, Y.; Leong, K. W. MicroRNA delivery for regenerative medicine. *Adv. Drug Delivery Rev.* **2015**, *88*, 108−122.

DOI: 10.1021/acs.molpharmaceut.6b00999
Mol. Pharmaceutics 2017, 14, 1395−1404

(5) Wang, H.; Jiang, Y.; Peng, H.; Chen, Y.; Zhu, P.; Huang, Y. Recent progress in microRNA delivery for cancer therapy by non-viral synthetic vectors. *Adv. Drug Delivery Rev.* **2015**, *81*, 142−60.
(6) Zhang, C.; Tang, N.; Liu, X.; Liang, W.; Xu, W.; Torchilin, V. P. siRNA-containing liposomes modified with polyarginine effectively silence the targeted gene. *J. Controlled Release* **2006**, *112*, 229−39.
(7) Chen, Y.; Zhu, X.; Zhang, X.; Liu, B.; Huang, L. Nanoparticles modified with tumor-targeting scFv deliver siRNA and miRNA for cancer therapy. *Mol. Ther.* **2010**, *18*, 1650−6.
(8) Grandinetti, G.; Ingle, N. P.; Reineke, T. M. Interaction of poly(ethylenimine)-DNA polyplexes with mitochondria: implications for a mechanism of cytotoxicity. *Mol. Pharmaceutics* **2011**, *8*, 1709−1719.
(9) Nam, K.; Jung, S.; Nam, J. P.; Kim, S. W. Poly(ethylenimine) conjugated bioreducible dendrimer for efficient gene delivery. *J. Controlled Release* **2015**, *220*, 447−55.
(10) Nelson, C. E.; Kintzing, J. R.; Hanna, A.; Shannon, J. M.; Gupta, M. K.; Duvall, C. L. Balancing cationic and hydrophobic content of PEGylated siRNA polyplexes enhances endosome escape, stability, blood circulation time, and bioactivity in vivo. *ACS Nano* **2013**, *7*, 8870−80.
(11) Geihe, E. I.; Cooley, C. B.; Simon, J. R.; Kiesewetter, M. K.; Edward, J. A.; Hickerson, R. P.; Kaspar, R. L.; Hedrick, J. L.; Waymouth, R. M.; Wender, P. A. Designed guanidinium-rich amphipathic oligocarbonate molecular transporters complex, deliver and release siRNA in cells. *Proc. Natl. Acad. Sci. U. S. A.* **2012**, *109*, 13171−6.
(12) Davis, M. E.; Zuckerman, J. E.; Choi, C. H.; Seligson, D.; Tolcher, A.; Alabi, C. A.; Yen, Y.; Heidel, J. D.; Ribas, A. Evidence of RNAi in humans from systemically administered siRNA via targeted nanoparticles. *Nature* **2010**, *464*, 1067−70.
(13) McLendon, J. M.; Joshi, S. R.; Sparks, J.; Matar, M.; Fewell, J. G.; Abe, K.; Oka, M.; McMurtry, I. F.; Gerthoffer, W. T. Lipid nanoparticle delivery of a microRNA-145 inhibitor improves experimental pulmonary hypertension. *J. Controlled Release* **2015**, *210*, 67−75.
(14) Zhang, Q.; Ran, R.; Zhang, L.; Liu, Y.; Mei, L.; Zhang, Z.; Gao, H.; He, Q. Simultaneous delivery of therapeutic antagomirs with paclitaxel for the management of metastatic tumors by a pH-responsive anti-microbial peptide-mediated liposomal delivery system. *J. Controlled Release* **2015**, *197*, 208−18.
(15) Hatakeyama, H.; Murata, M.; Sato, Y.; Takahashi, M.; Minakawa, N.; Matsuda, A.; Harashima, H. The systemic administration of an anti-miRNA oligonucleotide encapsulated pH-sensitive liposome results in reduced level of hepatic microRNA-122 in mice. *J. Controlled Release* **2014**, *173*, 43.
(16) Yang, Y. P.; Chien, Y.; Chiou, G. Y.; Cherng, J. Y.; Wang, M. L.; Lo, W. L.; Chang, Y. L.; Huang, P. I.; Chen, Y. W.; Shih, Y. H.; Chen, M. T.; Chiou, S. H. Inhibition of cancer stem cell-like properties and reduced chemoradioresistance of glioblastoma using microRNA145 with cationic polyurethane-short branch PEI. *Biomaterials* **2012**, *33*, 1462−76.
(17) Qian, X.; Long, L.; Shi, Z.; Liu, C.; Qiu, M.; Sheng, J.; Pu, P.; Yuan, X.; Ren, Y.; Kang, C. Star-branched amphiphilic PLA-b-PDMAEMA copolymers for co-delivery of miR-21 inhibitor and doxorubicin to treat glioma. *Biomaterials* **2014**, *35*, 2322−35.
(18) Gao, S.; Tian, H.; Guo, Y.; Li, Y.; Guo, Z.; Zhu, X.; Chen, X. miRNA oligonucleotide and sponge for miRNA-21 inhibition mediated by PEI-PLL in breast cancer therapy. *Acta Biomater.* **2015**, *25*, 184−93.
(19) Zhang, Y.; Buhrman, J. S.; Liu, Y.; Rayahin, J. E.; Gemeinhart, R. A. Reducible Micelleplexes are Stable Systems for Anti-miRNA Delivery in Cerebrospinal Fluid. *Mol. Pharmaceutics* **2016**, *13*, 1791−9.
(20) Dai, X.; Tan, C. Combination of microRNA therapeutics with small-molecule anticancer drugs: mechanism of action and co-delivery nanocarriers. *Adv. Drug Delivery Rev.* **2015**, *81*, 184−97.
(21) Chitkara, D.; Singh, S.; Mittal, A. Nanocarrier-based co-delivery of small molecules and siRNA/miRNA for treatment of cancer. *Ther. Delivery* **2016**, *7*, 245−55.
(22) Li, J.; Wang, Y.; Zhu, Y.; Oupicky, D. Recent advances in delivery of drug-nucleic acid combinations for cancer treatment. *J. Controlled Release* **2013**, *172*, 589−600.
(23) Gandhi, N. S.; Tekade, R. K.; Chougule, M. B. Nanocarrier mediated delivery of siRNA/miRNA in combination with chemotherapeutic agents for cancer therapy: current progress and advances. *J. Controlled Release* **2014**, *194*, 238−56.
(24) Costa, P. M.; Cardoso, A. L.; Custodia, C.; Cunha, P.; Pereira de Almeida, L.; Pedroso de Lima, M. C. MiRNA-21 silencing mediated by tumor-targeted nanoparticles combined with sunitinib: A new multimodal gene therapy approach for glioblastoma. *J. Controlled Release* **2015**, *207*, 31−9.
(25) Yao, C.; Liu, J.; Wu, X.; Tai, Z.; Gao, Y.; Zhu, Q.; Li, J.; Zhang, L.; Hu, C.; Gu, F.; Gao, J.; Gao, S. Reducible self-assembling cationic polypeptide-based micelles mediate co-delivery of doxorubicin and microRNA-34a for androgen-independent prostate cancer therapy. *J. Controlled Release* **2016**, *232*, 203−14.
(26) Dai, X.; Fan, W.; Wang, Y.; Huang, L.; Jiang, Y.; Shi, L.; McKinley, D.; Tan, W.; Tan, C. Combined Delivery of Let-7b MicroRNA and Paclitaxel via Biodegradable Nanoassemblies for the Treatment of KRAS Mutant Cancer. *Mol. Pharmaceutics* **2016**, *13*, 520−533.
(27) Zhang, N.; Huang, Y.; Wu, F.; Zhao, Y.; Li, X.; Shen, P.; Yang, L.; Luo, Y.; Yang, L.; He, G. Codelivery of a miR-124 Mimic and Obatoclax by Cholesterol-Penetratin Micelles Simultaneously Induces Apoptosis and Inhibits Autophagic Flux in Breast Cancer in Vitro and in Vivo. *Mol. Pharmaceutics* **2016**, *13*, 2466−83.
(28) Kumar, V.; Mondal, G.; Slavik, P.; Rachagani, S.; Batra, S. K.; Mahato, R. I. Codelivery of small molecule hedgehog inhibitor and miRNA for treating pancreatic cancer. *Mol. Pharmaceutics* **2015**, *12*, 1289−98.
(29) Dobrovolskaia, M. A.; McNeil, S. E. Immunological properties of engineered nanomaterials. *Nat. Nanotechnol.* **2007**, *2*, 469−478.
(30) Alouane, A.; Labruere, R.; Le Saux, T.; Schmidt, F.; Jullien, L. Self-immolative spacers: kinetic aspects, structure-property relationships, and applications. *Angew. Chem., Int. Ed.* **2015**, *54*, 7492−509.
(31) Shamis, M.; Lode, H. N.; Shabat, D. Bioactivation of self-immolative dendritic prodrugs by catalytic antibody 38C2. *J. Am. Chem. Soc.* **2004**, *126*, 1726−31.
(32) Niculescu-Duvaz, I.; Niculescu-Duvaz, D.; Friedlos, F.; Spooner, R.; Martin, J.; Marais, R.; Springer, C. J. Self-immolative anthracycline prodrugs for suicide gene therapy. *J. Med. Chem.* **1999**, *42*, 2485−9.
(33) Riber, C. F.; Smith, A. A.; Zelikin, A. N. Self-Immolative Linkers Literally Bridge Disulfide Chemistry and the Realm of Thiol-Free Drugs. *Adv. Healthcare Mater.* **2015**, *4*, 1887−90.
(34) Hu, X.; Hu, J.; Tian, J.; Ge, Z.; Zhang, G.; Luo, K.; Liu, S. Polyprodrug Amphiphiles: Hierarchical Assemblies for Shape-Regulated Cellular Internalization, Trafficking, and Drug Delivery. *J. Am. Chem. Soc.* **2013**, *135*, 17617−17629.
(35) Zhu, Y.; Li, J.; Kanvinde, S.; Lin, Z.; Hazeldine, S.; Singh, R. K.; Oupicky, D. Self-immolative polycations as gene delivery vectors and prodrugs targeting polyamine metabolism in cancer. *Mol. Pharmaceutics* **2015**, *12*, 332−41.
(36) Perissinotto, E.; Cavalloni, G.; Leone, F.; Fonsato, V.; Mitola, S.; Grignani, G.; Surrenti, N.; Sangiolo, D.; Bussolino, F.; Piacibello, W.; Aglietta, M. Involvement of chemokine receptor 4/stromal cell-derived factor 1 system during osteosarcoma tumor progression. *Clin. Cancer Res.* **2005**, *11*, 490−497.
(37) Wu, B.; Chien, E. Y.; Mol, C. D.; Fenalti, G.; Liu, W.; Katritch, V.; Abagyan, R.; Brooun, A.; Wells, P.; Bi, F. C.; Hamel, D. J.; Kuhn, P.; Handel, T. M.; Cherezov, V.; Stevens, R. C. Structures of the CXCR4 chemokine GPCR with small-molecule and cyclic peptide antagonists. *Science* **2010**, *330*, 1066−71.
(38) Fontanella, R.; Pelagalli, A.; Nardelli, A.; D'Alterio, C.; Ieranò, C.; Cerchia, L.; Lucarelli, E.; Scala, S.; Zannetti, A. A novel antagonist of CXCR4 prevents bone marrow-derived mesenchymal stem cell-mediated osteosarcoma and hepatocellular carcinoma cell migration and invasion. *Cancer Lett.* **2016**, *370*, 100−107.

DOI: 10.1021/acs.molpharmaceut.6b00999
Mol. Pharmaceutics 2017, 14, 1395−1404

(39) Rosenkilde, M. M.; Gerlach, L.-O.; Hatse, S.; Skerlj, R. T.; Schols, D.; Bridger, G. J.; Schwartz, T. W. Molecular mechanism of action of monocyclam versus bicyclam non-peptide antagonists in the CXCR4 chemokine receptor. *J. Biol. Chem.* **2007**, *282*, 27354−27365.
(40) Ling, X.; Spaeth, E.; Chen, Y.; Shi, Y.; Zhang, W.; Schober, W.; Hail, N.; Konopleva, M.; Andreeff, M. The CXCR4 antagonist AMD3465 regulates oncogenic signaling and invasiveness in vitro and prevents breast cancer growth and metastasis in vivo. *PLoS One* **2013**, *8*, e58426.
(41) Kopeček, J.; Kopečková, P. HPMA copolymers: Origins, early developments, present, and future. *Adv. Drug Delivery Rev.* **2010**, *62*, 122−149.
(42) Li, J.; Oupický, D. Effect of biodegradability on CXCR4 antagonism, transfection efficacy and antimetastatic activity of polymeric Plerixafor. *Biomaterials* **2014**, *35*, 5572−5579.
(43) Wang, Y.; Hazeldine, S. T.; Li, J.; Oupický, D. Development of functional poly(amido amine) CXCR4 antagonists with the ability to mobilize leukocytes and deliver nucleic acids. *Adv. Healthcare Mater.* **2015**, *4*, 729−738.
(44) Roth, P. J.; Boyer, C.; Lowe, A. B.; Davis, T. P. RAFT polymerization and thiol chemistry: a complementary pairing for implementing modern macromolecular design. *Macromol. Rapid Commun.* **2011**, *32*, 1123−43.
(45) Xie, Y.; Wehrkamp, C. J.; Li, J.; Wang, Y.; Wang, Y.; Mott, J. L.; Oupický, D. Delivery of miR-200c Mimic with Poly(amido amine) CXCR4 Antagonists for Combined Inhibition of Cholangiocarcinoma Cell Invasiveness. *Mol. Pharmaceutics* **2016**, *13* (3), 1073−1080.
(46) Tiram, G.; Segal, E.; Krivitsky, A.; Shreberk-Hassidim, R.; Ferber, S.; Ofek, P.; Udagawa, T.; Edry, L.; Shomron, N.; Roniger, M.; Kerem, B.; Shaked, Y.; Aviel-Ronen, S.; Barshack, I.; Calderón, M.; Haag, R.; Satchi-Fainaro, R. Identification of Dormancy-Associated MicroRNAs for the Design of Osteosarcoma-Targeted Dendritic Polyglycerol Nanopolyplexes. *ACS Nano* **2016**, *10*, 2028−2045.
(47) Zhang, J.; Ma, L. MicroRNA control of epithelial−mesenchymal transition and metastasis. *Cancer Metastasis Rev.* **2012**, *31*, 653−662.
(48) Lamouille, S.; Xu, J.; Derynck, R. Molecular mechanisms of epithelial−mesenchymal transition. *Nat. Rev. Mol. Cell Biol.* **2014**, *15*, 178−196.
(49) Ma, C.; Huang, T.; Ding, Y.-C.; Yu, W.; Wang, Q.; Meng, B.; Luo, S.-X. microRNA-200c overexpression inhibits chemoresistance, invasion and colony formation of human pancreatic cancer stem cells. *Int. J. Clin. Exp. Pathol.* **2015**, *8*, 6533−6539.
(50) Jurmeister, S.; Baumann, M.; Balwierz, A.; Keklikoglou, I.; Ward, A.; Uhlmann, S.; Zhang, J. D.; Wiemann, S.; Sahin, Ö. MicroRNA-200c Represses Migration and Invasion of Breast Cancer Cells by Targeting Actin-Regulatory Proteins FHOD1 and PPM1F. *Mol. Cell. Biol.* **2012**, *32*, 633−651.

DOI: 10.1021/acs.molpharmaceut.6b00999
Mol. Pharmaceutics 2017, 14, 1395−1404